Inorganica Chimica Acta, 146 (1988) 173–180

FT-IR and XPS Study of Copper(II) Complexes of Imidazole and Benzimidazole

DENIS P. DROLET, DAVID M. MANUTA, ALISTAIR J. LEES*

Department of Chemistry, University Center at Binghamton, State University of New York, Binghamton, N.Y. 13901, U.S.A.

A. D. KATNANI

IBM Corporation, Endicott, N.Y. 13760, U.S.A.

and GEORGE J. COYLE

IBM Corporation, East Fishkill, N.Y. 12524, U.S.A.

(Received September 30, 1987)

Abstract

Several Cu(II) complexes coordinated to imidazole (IMDAH) and benzimidazole (BIMDAH) ligands have been isolated as powdered solids. Compounds prepared are $Cu(BIMDAH)_4Cl_2$, $Cu(IMDAH)_4Cl_2$, $Cu(BIMDAH)_2Cl_2$, $Cu(IMDAH)_2Cl_2$ and $Cu(BIMDA)_2$ (BIMDA = deprotonated form of BIMDAH ligand). These compounds have been characterized by elemental analysis, and by diffuse reflectance Fourier Transform and X-ray photoelectron spectroscopy. The results show that $Cu(BIMDAH)_4Cl_2$ and $Cu(IMDAH)_4Cl_2$ are formed as discrete mononuclear complexes in which the ligands are coordinated in a monodentate fashion. In contrast, the $Cu(BIMDAH)_2Cl_2$ and $Cu(IMDAH)_2Cl_2$ complexes are formed as polymeric species. The $Cu(BIMDA)_2$ complex also forms a polymeric structure with the ligands coordinated in a bidentate manner. X-ray photoelectron data illustrates that the surface composition of each of these complexes closely resembles that of the bulk material.

Introduction

Azoles, such as benzotriazole (BTAH), imidazole (IMDAH), and benzimidazole (BIMDAH) are used extensively in industrial processes as corrosion inhibitors for metal and alloy surfaces, particularly that of copper [1, 2]. The nature of the passivating film on copper has been studied by a variety of experimental techniques including infrared spectroscopy [2], X-ray photoelectron spectroscopy [3, 4] and ellipsometry [5]. Nevertheless, the important features of bonding and growth of the passivating film are not fully characterized. In surface films of benzotriazole on copper metal both Cu(I)–BTA and Cu(II)–BTA (BTA = the deprotonated form of the benzotriazole ligand) complexes are thought to be present [4, 6].

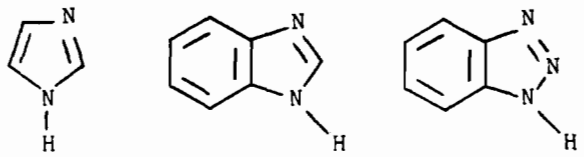

imidazole (IMDAH) | benzimidazole (BIMDAH) | benzotriazole (BTAH)

The coordination chemistry of azoles acting as ligands in copper(II) compounds has also been studied in the context of modeling biological systems. Cu(II)–imidazole bonding has been observed in the histidine containing plastocyanin [7] and azurin peptides [8]. Extensive studies of the electronic spectra of $Cu(IMDAH)_4^{2+}$ and closely related substituted imidazole complexes have aided in the characterization of these peptide systems [9–11]. Studies of the coordination chemistry of azoles acting as ligands in copper compounds have proven difficult, largely because of the insoluble nature of many of these complexes. Also, these complexes are typically formed as powders and are, therefore, not conducive to single crystal determination. Moreover, these compounds are apparently able to bond in a variety of modes (e.g. the BTA ligand may coordinate in unidentate, bidentate, or tridentate forms) and the synthesis and characterization of unique compounds to serve as bonding models has been problematic.

This article reports our preparation of several copper(II) compounds involving imidazole and benzimidazole ligands. The reactivity of these ligands and the compounds they form with $CuCl_2$ serve as

*Author to whom correspondence should be addressed.

0020-1693/88/$3.50

models for the varied BTAH/$CuCl_2$ chemistry that has been observed by other researchers [12–14]. The bulk composition and bonding of these compounds have been characterized by elemental analysis and diffuse reflectance Fourier Transform infrared (FT-IR) spectroscopy. Additionally, the surface chemistry has been investigated by X-ray photoelectron (XPS) spectroscopy.

Experimental

Materials

$CuCl_2$ was obtained from Aldrich Chemical Co. and used without further purification. Benzimidazole (BIMDAH) and imidazole (IMDAH) were also obtained from Aldrich Chemical Co. and sublimed before use. Ethanol was dried and stored over potassium carbonate.

Preparation of Compounds

All compounds were synthesized in solution at ambient temperature. Discrete products were only obtained at 1:2 and 1:4 metal:ligand ratios. Complexes $Cu(BIMDAH)_2Cl_2$ and $Cu(IMDAH)_2Cl_2$ were prepared by reacting cupric chloride (2 mmol) and appropriate ligand (4 mmol) in dry ethanol (80 ml). The $Cu(BIMDAH)_4Cl_2$ and $Cu(IMDAH)_4Cl_2$ compounds were prepared by reacting cupric chloride (1 mmol) and appropriate ligand (4 mmol) in dry ethanol (100 ml). The $Cu(BIMDA)_2$ and $Cu(IMDA)_2$ compounds were synthesized by reaction of cupric chloride (2 mmol) with ligand (4 mmol) in 0.1 M NaOH solution with constant stirring. Each complex was obtained by vacuum filtration and purified by repeated ethanol washings and subsequently dried in vacuum for a minimum of 12 h. Obtained yields and melting points are $Cu(BIMDAH)_2Cl_2$ (78%, 167–169 °C), $Cu(IMDAH)_2Cl_2$ (84%, 190–193 °C), $Cu(BIMDAH)_4Cl_2$ (77%, 194 °C), $Cu(IMDAH)_4Cl_2$ (91%, 213–216 °C), $Cu(BIMDA)_2$ (74%, 280 °C dec.). The compounds were analyzed for Cu by iodometric determination [15]; analyses for carbon, hydrogen, and nitrogen were determined via combustion techniques performed by MICANAL, Inc. of Tucson, Arizona.

Physical Measurements

Infrared spectra were recorded from samples as finely ground powders with a Spectra-Tech diffuse-reflectance attachment on a Nicolet 20SXC Spectrophotometer. Although the instrumental resolution is ±0.1 cm^{-1}, in practice, spectral resolution was found to be limited by particle size and the reported band maxima are considered accurate to ±0.5 cm^{-1}. Diffuse reflectance spectra were analyzed using Kubelka–Munk theory (see eqn. (1)) [16].

$$f(R) = \frac{(1-R)^2}{2R} = \frac{K}{S} \quad (1)$$

Here R is the measured reflectance, and K and S are the absorption and scattering constants, respectively. The conversion to Kubelka–Munk units was carried out with the Nicolet SX software.

XPS spectra were obtained using a XSAM-800 Kratos spectrometer from powder samples that were spread on an indium foil. Al Kα or Mg Kα radiation was used to excite photoelectrons from the Cu(2p), C(1s), Cl(2p), and N(1s) core levels. Effects of sample charging were determined from the observed shifts in the C–H contribution to the C(1s) lineshape. Typically, these shifts were 2–4 eV and did not appreciably affect the core level lineshapes. The overall energy resolution was estimated from the $Ag(3d_{5/2})$ emission line to be 0.9 eV. A least-squares fitting technique that employs Gaussian functions was used to deconvolute the XPS lineshapes. The fitting parameters were kept free for each of the core levels, except for the Cl(2p) lineshape where the branching ratio was fixed at $2p_{3/2}/2p_{1/2} = 2$. The probe depth in these XPS experiments is in the range 10–50 Å.

Results

Synthesis

Discrete copper–imidazole and copper–benzimidazole complexes were obtained following synthesis at 1:2 or 1:4 metal:ligand ratios. Virtually no reaction took place with a 1:1 metal:ligand ratio. At a 1:3 metal:ligand reagent ratio a mixture of the above 1:2 and 1:4 products was formed. At metal:ligand ratios of 1:5 and 1:6 the reaction was incomplete as evidenced by unreacted ligand material remaining in the reaction vessel. A list of all synthesized compounds, including their colors and elemental analyses (Cu, C, H, N) is presented in Table I.

FT-IR Spectra

Diffuse reflectance Fourier Transform infrared spectra (DR-FT-IR) recorded between 4000–500 cm^{-1} for the $Cu(BIMDAH)_2Cl_2$, $Cu(BIMDAH)_4Cl_2$, and $Cu(BIMDA)_2$ complexes and the free BIMDAH ligand are depicted in Fig. 1. DR-FT-IR data obtained from all the complexes studied and the free ligands themselves are listed in Tables II and III. Assignments for the complexes are based on a force constant analysis performed on the free ligands [17].

XPS Spectra

Figure 2 shows the Cu(2p) and Cl(2p) emission lines from the $Cu(BIMDAH)_2Cl_2$, $Cu(BIMDAH)_4Cl_2$ and $Cu(BMIDA)_2$ complexes. The Cu(2p) lineshape indicates that Cu is present only as Cu(+2) ions as

TABLE I. Elemental Analyses and Colors of Copper(II)–Azole Compounds

Compound	Cu (%)		C (%)		H (%)		N (%)		Color
	Calc.	Found	Calc.	Found	Calc.	Found	Calc.	Found	
$Cu(BIMDAH)_2Cl_2$	17.14	17.26	45.35	45.92	3.27	3.26	15.11	15.29	green
$Cu(BIMDAH)_4Cl_2$	10.47	9.98	55.40	54.69	3.99	4.49	18.45	17.53	blue
$Cu(BIMDA)_2$	21.34	21.00	56.46	56.75	3.39	3.46	18.80	18.82	brick red
$Cu(IMDAH)_2Cl_2$	23.48	23.41	26.63	26.96	2.99	3.02	20.69	20.07	green
$Cu(IMDAH)_4Cl_2$	16.62	16.14	35.43	33.56	3.97	3.73	27.54	26.50	dark blue

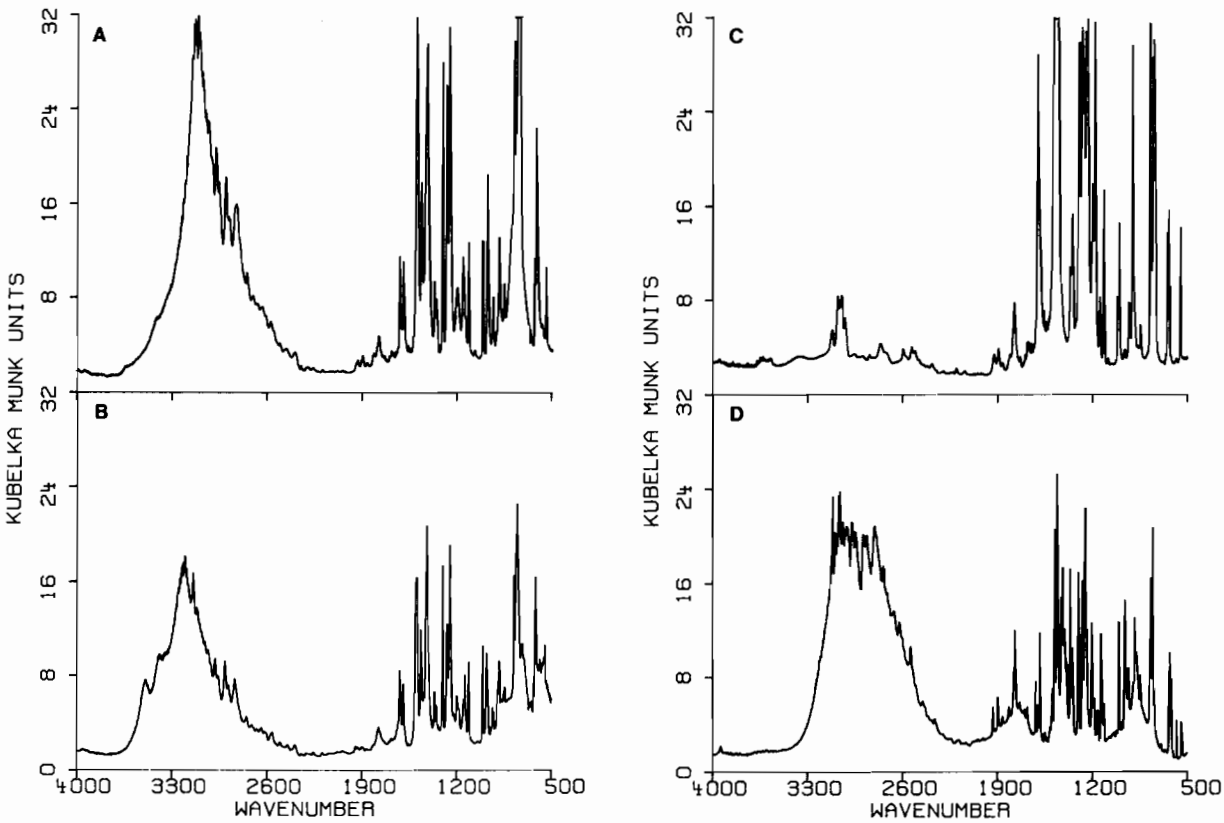

Fig. 1. Diffuse reflectance Fourier Transform infrared spectra in the 4000–500 cm^{-1} region for (A) $Cu(BIMDAH)_4Cl_2$, (B) $Cu(BIMDAH)_2Cl_2$, (C) $Cu(BIMDA)_2$ and (D) BIMDAH ligand.

the shakeup satellites present at binding energies of 942.7 and 962.0 eV are characteristic of the unfilled d-orbitals. The Cl(2p) lineshapes were, in each case, fitted to two Gaussian functions separated by 0.5 eV, with a peak ratio of 1:2; this result demonstrates that in each complex the Cl atoms are present in only one bonding configuration.

Table IV lists the binding energies obtained from the Cu(2p), C(1s), N(1s) and Cl(2p) levels of the complexes. The calculated atomic ratios C/N, N/Cu and Cl/Cu are also included; the errors associated with these ratios depend on several parameters [18] and are estimated to be within ±20%. It is noted that the C/N ratios of the complexes reflect the expected atomic ratios for the corresponding free ligands. The Cu(2p) binding energy was found to be independent of the metal:ligand ratio, although it does depend on the ligand used.

Discussion

$Cu(BIMDAH)_2Cl_2$

Elemental analyses obtained from this green complex are consistent with the above empirical formula (see Table I). DR-FT-IR spectra recorded from the complexes in the 4000–500 cm^{-1} range illustrate that the BIMDAH ligand vibrations are slightly shifted

TABLE II. Diffuse Reflectance FT-IR Spectra of BIMDAH and Cu(II) Complexes[a]

BIMDAH	$Cu(BIMDAH)_4Cl_2$	$Cu(BIMDAH)_2Cl_2$	$Cu(BIMDA)_2$	Assignments
		3205(w)		
		3144(w)		
	3139(m)			
	3127(m)			
3113(w)	3109(m)	3118(w)	3118(w)	
3095(w)	3098(m)			
			3076(m)	
3061(w)			3048(m)	
3038(w)	3036(m)	3035(m)		
			3024(w)	
3011(w)				CH stretching and
2973(w)	2979(w)	2982(w)		NH stretching
2969(w)				
	2957(w)	2962(w)		
2949(w)				
2944(w)				
	2907(w)	2910(w)		
2889(w)	2884(w)	2885(w)		
2865(w)				
	2828(w)	2839(w)		
2804(w)				
	2751(w)	2752(w)		
2624(w)				
2541(w)				
1934(w)				1005 + 933
			1926(w)	
1898(w)			1895(w)	overtone
1817(w)			1810(sh)	overtone
1772(m)	1778(w)	1776(w)	1778(m)	overtone
1620(w)	1623(m)	1623(m)		ring stretching
1601(w)			1606(s)	
	1594(m)	1597(m)		N–H inplane bending
1588(m)				
		1506(m)		756 + 744
1495(w)	1497(s)	1496(m)		
1478(m)			1474(s)	
1462(m)	1464(m)	1466(m)		
			1455(s)	
1420(m)	1422(s)	1423(s)		ring stretching
1406(m)				
1366(m)	1365(m)	1364(w)	1364(m)	
1350(w)	1351(m)	1352(w)	1349(m)	
1346(m)				
1303(m)	1305(s)	1305(s)	1300(s)	ring stretching
1276(m)	1275(s)	1273(m)	1276(m)	
1272(m)				Bz. inplane bending
			1264(m)	
1252(s)	1253(s)	1250(m)		
			1239(s)	ring stretching
1203(m)	1196(m)	1198(w)	1201(m)	
1187(w)		1187(sh)	1183(s)	
1159(w)				Bz. inplane CH bending
1153(w)	1154(m)			
		1148(w)	1148(m)	
1136(m)	1137(w)	1139(m)		N–H inplane bending
1113(w)	1113(m)	1110(m)	1119(m)	Bz. CH inplane bending
			1017(m)	
1005(m)	1009(m)	1009(m)	1006(m)	Bz. inplane ring bending

(continued)

TABLE II. *(continued)*

BIMDAH	$Cu(BIMDAH)_4Cl_2$	$Cu(BIMDAH)_2Cl_2$	$Cu(BIMDA)_2$	Assignments
	975(m)	979(m)		
			966(w)	Im. CH inplane bending
960(m)				
933(m)	931(m)	934(w)	932(m)	Bz. inplane ring bending
			907(s)	
888(m)	888(m)	887(m)		Im. inplane ring bending
848(m)	850(m)	846(w)	848(w)	Im. CH outplane bending
	779(s)	778(m)	776(s)	
770(m)	764(s)	765(m)	768(m)	Im. plane ring bending
		761(s)		
756(s)		759(s)		
	750(s)		752(s)	Bz. CH outplane bending
744(m)				
		716(s)		
			650(m)	
635(m)	633(m)	635(m)	639(m)	Im. ring torsion
627(m)				NH outplane bending
618(m)	621(s)	618(m)		inplane ring bending
		585(m)		
579(w)				
			553(m)	ring torsion
544(m)	548(m)	548(m)		

[a]Band intensities: s = strong, m = medium, w = weak, sh = shoulder.

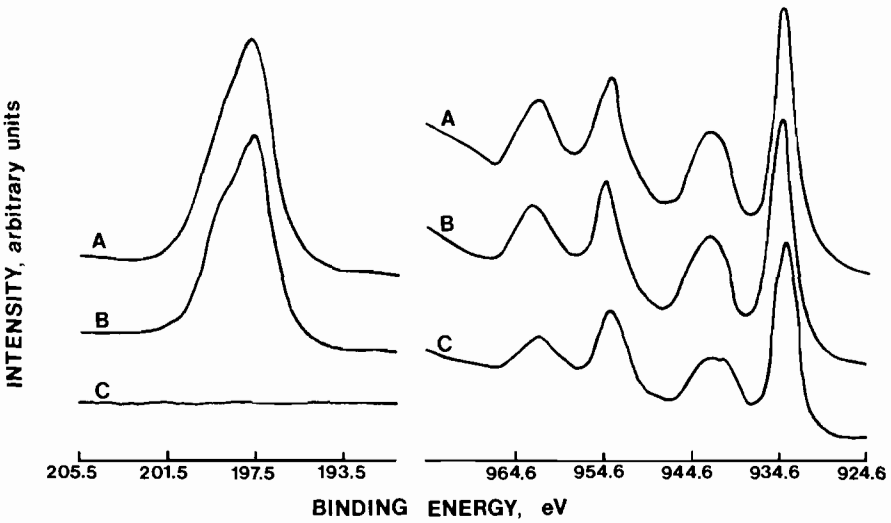

Fig. 2. XPS Cu(2p) and Cl(2p) emission lines obtained from (A) $Cu(BIMDAH)_4Cl_2$, (B) $Cu(BIMDAH)_2Cl_2$ and (C) $Cu(BIMDA)_2$.

from those of the free ligand (see Fig. 1 and Table II). The presence of N–H stretching and N–H bending modes indicate that the ligand proton remains bound at the N1 position and, thus, the metal to ligand bonding takes place at the N2 position. The elemental analysis and FT-IR spectroscopic data are consistent with the polymeric structure below. In addition, the XPS data in Table IV indicate that the Cu center has formally a +2 charge, that the C/N atomic ratio of this complex reflects that of the free ligand, and that the Cl/Cu and N/Cu atomic ratios are, within experimental uncertainty, in accordance with the proposed polymeric structure. Moreover, the XPS results illustrate that the surface composition of this compound is essentially identical to that of the bulk material.

$Cu(IMDAH)_2Cl_2$

Elemental analyses, FT-IR and XPS data obtained from this pale green complex illustrate that its

TABLE III. Diffuse Reflectance FT-IR Spectra of IMDAH and Cu(II) Complexes[a]

IMDAH	$Cu(IMDAH)_4Cl_2$	$Cu(IMDAH)_2Cl_2$	Assignments
		3338(m)	
	3299(w)		
	3293(w)		
	3156(m)		
	3143(m)	3145(m)	
		3135(m)	
3126(m)	3123(m)	3126(m)	CH stretching
	3064(m)	3063(m)	and
	3059(w)		NH stretching
3051(w)			
	2955(m)	2956(m)	
2935(s)			
2876(w)			
	2851(m)	2851(m)	
	2608(w)		
	2578(w)		
1669(m)			2 × 832
1577(w)			CC stretching
1558(w)			
1540(m)	1540(s)	1543(s)	NH bending
	1506(s)	1506(m)	
1500(m)			
	1496(m)	1496(m)	
1490(m)	1490(m)		
1482(m)			
	1476(m)	1476(w)	
	1472(m)	1473(w)	
1452(m)	1457(m)	1457(w)	
	1437(m)		ring stretching
	1430(m)	1430(m)	
	1424(m)	1424(m)	
	1419(m)	1419(m)	
	1339(m)	1334(m)	
1329(m)	1329(m)	1329(m)	CH bending
1266(m)			ring breathing
1260(m)	1262(m)	1262(m)	
	1255(m)	1253(m)	
1245(m)	1245(m)		656 + 592 (Raman)
	1225(w)	1230(w)	
1175(w)	1174(m)	1174(m)	
	1165(m)		
1149(m)			NH bending
	1142(m)	1143(m)	
1139(m)			
	1128(m)	1127(m)	
	1113(m)	1114(sh)	
		1108(m)	
1099(m)	1095(m)	1095(s)	CH bending
	1807(m)		
1068(m)	1074(s)	1071(s)	
1046(w)			
	954(m)	954(m)	
946(m)	944(m)	944(m)	
923(m)	921(m)	920(m)	ring bending
899(m)	874(m)	873(m)	
			861(m)	857(m)	
			843(m)	846(m)	
832(m)				828(m)	
			807(m)	806(m)	
			804(m)		
			783(m)		
				772(s)	
			759(m)	759(s)	γ CH
743(m)			749(m)	749(s)	
			679(m)		
668(w)			668(s)	666(s)	
657(w)			653(m)	656(sh)	torsion mode
623(m)			623(m)	623(sh)	NH out of plane bending
			612(m)	615(s)	
				565(m)	

[a]Band intensities: s = strong, m = medium, w = weak, sh = shoulder.

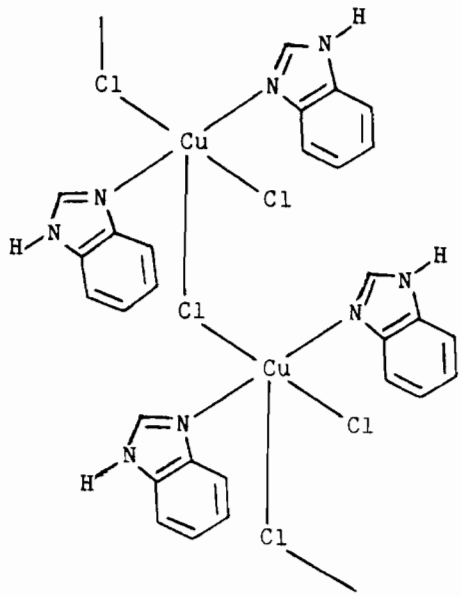

coordination is essentially identical to that in the above $Cu(BIMDAH)_2Cl_2$ complex (see Tables, I, III, and IV).

$Cu(BIMDAH)_4Cl_2$

Elemental analyses are consistent with this blue compound having the above empirical formula (see Table I). As in the previous complexes, FT-IR spectra indicate that the N–H stretching and N–H bending modes are still observable for the coordinated ligand (see Fig. 1 and Table II). Therefore, the BIMDAH ligand must be bonded to the metal via the N2 atom. The presence of only Cu(+2) features in the XPS

TABLE IV. Binding Energies and Relative Atomic Ratios for Cu(2p), Cl(2p), C(1s), and N(1s) Core Levels of the Various Copper–Azole Complexes[a]

Compound	Binding energy (eV)				Atomic ratio		
	Cu(2p)	C(1s)	N(1s)	Cl(2p)	Cl/Cu	N/Cu	C/N
$Cu(BIMDAH)_2Cl_2$	935.6	285.0	399.6	198.3	2.0	4.1	3.5
$Cu(BIMDAH)_4Cl_2$	935.6	285.0	399.6	198.1	2.3	7.0	3.5
$Cu(BIMDA)_2$	935.9	285.0	399.2			4.0	3.5
$Cu(IMDAH)_2Cl_2$	935.3	285.0	399.3	197.7	2.3	4.2	1.6
$Cu(IMDAH)_4Cl_2$	935.3	285.0	399.3	197.7	2.5	7.0	1.6

[a]Experimental uncertainty within ± 0.10 eV and ± 20%, respectively.

spectra supports the $Cu(BIMDAH)_4Cl_2$ formula. Also, the C/N, Cl/Cu and N/Cu XPS results imply that the surface composition of the $Cu(BIMDAH)_4Cl_2$ complex is very like that of the bulk material. The spectroscopic and analysis data are consistent with the following bonding model involving monodentate ligand coordination.

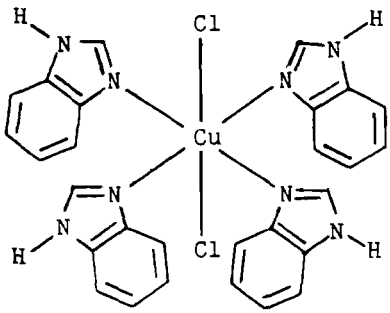

$Cu(IMDAH)_4Cl_2$

The experimental results obtained on this dark blue compound are consistent with the empirical formula $Cu(IMDAH)_4Cl_2$ (see Table I). This and the recorded DR-FT-IR and XPS spectroscopic data illustrate that the ligand coordination is essentially the same as in the $Cu(BIMDAH)_4Cl_2$ complex.

$Cu(BIMDA)_2$

This complex was prepared from a basic solution (see 'Experimental') and characterized to have the above empirical formula by elemental analyses (see Table I). DR-FT-IR data shown in Fig. 1 (compare spectra C and D) and Table II indicate an absence of the N–H stretching and N–H bending modes for this molecule. These results imply that the ligand is coordinated to the metal via both the N1 and N2 atoms in this complex. Qualitatively the rate at which the red product complex is formed depends substantially on the pH, increasing as the solution becomes more basic. Additionally, dilute aqueous solutions of either the green $Cu(BIMDAH)_2Cl_2$ complex or the blue $Cu(BIMDAH)_4Cl_2$ complex will react to form the red $Cu(BIMDA)_2$ complex. All of these observations above suggest that the deprotonated form BIMDA is involved in the coordination. Importantly, XPS data confirm the +2 oxidation state of the metal center but illustrate that chloro ligands are not present in the complex (see Fig. 2). The Cu/N and C/N atomic ratios are consistent with the elemental analysis values obtained from the bulk material. Additionally, it is noted that the binding energy of this complex increases by 0.3 eV for the Cu(2p) emission line and decreases by 0.4 eV for the N(1s) line; these changes in charge distribution further signify that this complex has a substantially different coordination geometry. The following structure is proposed on the basis of the above experimental results.

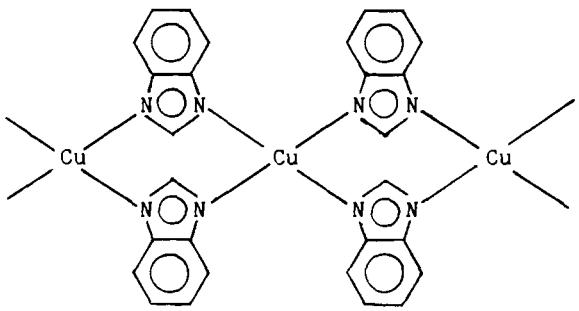

$Cu(IMDA)_2$

Efforts to synthesize the deprotonated $Cu(IMDA)_2$ complex were unsuccessful. The granular gray–green precipitate proved to be a complex mixture. The difficulty in isolating a pure product may be due to the increased basicity [18] of the N1 proton for IMDAH ($pK_a = 7.25$) compared to BIMDAH ($pK_a = 5.53$) which must be removed prior to bidentate coordination. Further spectroscopic measurements were not carried out for this complex.

Conclusions

A combination of diffuse-reflectance Fourier Transform and X-ray photoelectron spectroscopic

techniques have been used to characterize bonding for several copper complexes with imidazole and benzimidazole ligands. At metal:ligand ratios of 1:2 and 1:4, respectively, polynuclear and mononuclear species have been obtained; the bonding geometries determined for each of these compounds are independent of the ligand used. Treatment of these 1:2 and 1:4 Cu–BIMDAH complexes in basic solution results in the formation of bridged complexes in which the chloro ligands are dissociated. Importantly, the agreement between XPS and elemental analysis results illustrates the absence of any fragmentation or reconstruction on the surfaces of any of these complexes.

Acknowledgements

We are grateful to IBM Corporation for its support of this research and thank Dr Donald P. Seraphim for several useful discussions.

References

1 I. Dugdale and J. B. Cotton, *Corr. Sci., 3,* 69 (1963); J. Cotton and I. R. Scholes, *Br. Corr. J., 2,* 1 (1967); R. W. Walker, *Anticorrosion, 17,* 9 (1970).

2 G. Poling, *Corr. Sci., 10,* 359 (1970); S. Thiboult, *Corr. Sci., 17,* 701 (1977).

3 R. F. Roberts, *J. Electron Spectrosc. Relat. Phenom., 4,* 273 (1976); D. Chadwick and T. Hashemi, *J. Electron Spectrosc. Relat. Phenom., 10,* 79 (1977).

4 D. Chadwick and T. Hashemi, *Corr. Sci., 18,* 39 (1978); A. R. Siedle, R. A. Velapoldi and N. Erickson, *Appl. Surf. Sci., 3,* 229 (1979); H. G. Thompkins and S. P. Sharma, *Surf. Interf. Anal., 4,* 261 (1982).

5 N. D. Hobbins and R. F. Roberts, *Surf. Technol., 9,* 235 (1979).

6 I. C. G. Ogle and G. W. Polling, *Can. Metall. Quart., 14,* 37 (1975).

7 P. M. Coleman, H. C. Freeman, J. M. Guss, M. Murata, V. A. Norris, J. A. M. Ramshaw and M. P. Venhatappa, *Nature (London), 272,* 319 (1980).

8 E. T. Adman, R. E. Steinkamp, L. C. Sieker and L. H. Jensen, *J. Mol. Biol., 123,* 35 (1978).

9 T. G. Fawcett, E. E. Bernarducci, K. Krogh-Jespersen and H. J. Schugar, *J. Am. Chem. Soc., 102,* 2598 (1980).

10 E. E. Bernarducci, W. F. Schwindinger, J. L. Hughey, K. Krogh-Jespersen and H. J. Schugar, *J. Am. Chem. Soc., 103,* 1686 (1981).

11 E. E. Bernarducci, P. K. Bhardwaj, K. Krogh-Jespersen, J. A. Potenza and H. J. Schugar, *J. Am. Chem. Soc., 105,* 3860 (1983).

12 J. Reedijk, A. R. Siedle, R. A. Velapoldi and J. A. M. Van Hest, *Inorg. Chim. Acta, 74,* 109 (1983).

13 G. Ivarsson, *Acta Chem. Scand., 27,* 3523 (1973).

14 B. K. S. Lundberg, *Acta Chem. Scand., 26,* 3977 (1972).

15 C. Lewis and D. A. Skoog, *J. Am. Chem. Soc., 84,* 1101 (1962).

16 H. G. Hecht, *Appl. Spectrosc., 37,* 348 (1983); R. W. Frei and J. D. MacNeil, 'Diffuse Reflectance Spectroscopy in Environmental Problem-Solving', CRC Press, West Palm Beach, Fla., 1973.

17 M. Cordes and J. L. Walter, *Spectrochim. Acta, Part A, 24,* 237 (1968); M. Cordes and J. L. Walter, *Spectrochim. Acta, Part A, 24,* 1421 (1968); D. G. Sullivan, *J. Chem. Soc.,* 3653 (1960).

18 J. Cazaux, *J. Microsc. Spectrosc. Electron, 10,* 583 (1985), and refs therein.

19 A. R. Katritzky and C. W. Rees, 'Comprehensive Heterocyclic Chemistry', Vol. 5, Part 4a, Pergamon Press, Exeter, U.K., 1984, pp. 384–385.